

# Fabrication of oxide nanostructures on glass by aluminum anodization and sol–gel process

S.Z. Chu\*, K. Wada, S. Inoue, S. Todoroki

*Advanced Materials Lab., National Institute for Materials Science, Namiki 1-1, Tsukuba, Ibaraki 305-0044, Japan*

## Abstract

A novel process of fabricating various oxide nanostructures on glass substrates is described. Transparent porous alumina films ( $\varnothing$  6–150 nm) were first formed in acid solutions by anodization of aluminum layers sputter-deposited on a glass plate coated with a tin-doped indium oxide film. The porous alumina structures after pore-widened were then used as a host or a template in a sol–gel process to synthesize hollow or solid titania nanostructures within the nanopores, depending on the pore size of films and the affinity of the  $\text{TiO}_2$  gel to alumina films. Finally, titania nanotubules ( $\sim\varnothing$  200 nm) or nanofibers ( $\sim\varnothing$  50 nm) arrays on glass were fabricated after the anodic alumina films were selectively removed.  
© 2003 Elsevier Science B.V. All rights reserved.

**Keywords:** Titania nanotubules and nanofibers; Aluminium anodization; Sol–gel process

## 1. Introduction

Nanostructured materials have attracted a great interest in their potential applications in various fields such as electronics, magnetism, optics and energy storage or exchange, etc. A variety of nanostructures (nanotubules, nanofibers) had been synthesized upon a template-method [1,2] using commercial porous alumina membranes produced by anodization of aluminum plates or foils [3,4]. However, many concrete problems such as assembly and recycling of the nanostructures in manufacturing practical devices have not been well solved yet. Therefore, in the present study, we tried to create a novel nanotechnology to fabricate various nanostructures directly on glass substrates by combining anodization of sputtered aluminum with a sol–gel process. This technology is expected to be applied in manufacturing practical devices or functional glass for photocatalysis and/or solar energy systems.

## 2. Experimental

The fabrication procedure of oxide nanostructures on glass is schematically shown in Fig. 1: aluminum is first deposited on a glass substrate with a transparent and

conductive tin-doped indium oxide (ITO) film (a); a porous alumina structure is then formed on the glass substrate by anodization (b); after pore-widening to enlarge the pores and remove the barrier layer, the porous alumina structure is used as a host or a template to synthesize various  $\text{TiO}_2$  materials (hollow or solid) within the nanopores by a sol–gel process, forming an alumina–titania composite layer (c); various nanostructures (tubules or fibers) on glass substrates are finally fabricated after the anodic alumina is removed by selective chemical etching (d).

Highly pure aluminum film (99.99%, 1.5–2.0  $\mu\text{m}$ ) deposited on a soda lime glass substrate with an ITO (10  $\Omega/\square$ ,  $\sim$ 100 nm) film by a RF-sputtering was used as specimens. Anodization was carried out potentiostatically in solutions of phosphoric (10%, 60–150 V, 277–283 K), oxalic (3%, 40 V, 293 K) or sulfuric (10%, 15 V, 283 K) acid, respectively. To enlarge the pore size, the anodized specimens were immersed in a 5% phosphoric acid solution for 5–45 min. In sol–gel coating, the porous alumina structures were first dipped in a  $\text{TiO}_2$  sol ( $\sim$ 5% wt.) at room temperature for 10–20 min and then heated at 673 K for 2 h for the crystallization of anatase  $\text{TiO}_2$ . Details for the synthesis method of  $\text{TiO}_2$  sol were described elsewhere [5]. Titania nanotubules arrays on glass were achieved by mechanical abrasion and chemical etching in a solution of 5%  $\text{H}_3\text{PO}_4$  and 3%  $\text{CrO}_3$  at 353 K for 5 min.

\*Corresponding author. Tel.: +81-298-51-3354; fax: +81-298-54-9060.

E-mail address: [chu.songzhu@nims.go.jp](mailto:chu.songzhu@nims.go.jp) (S.Z. Chu).

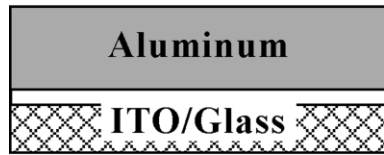
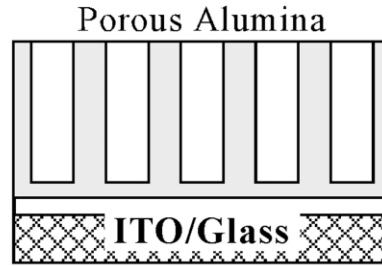
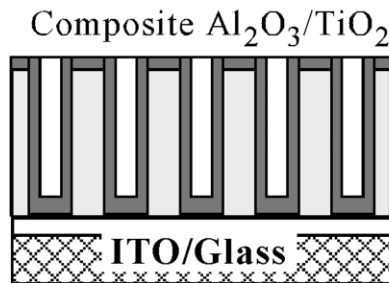
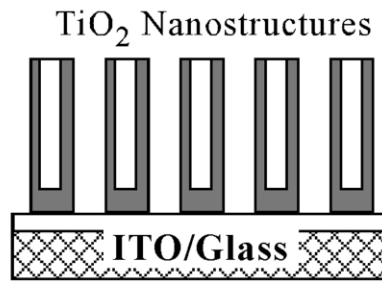
**a) RF-Sputtering:****b) Al Anodizing:****c) Sol-Gel Coating:****d) Selective Etching:**

Fig. 1. Scheme of fabrication procedure of nanostructures on ITO/glass substrates.

The morphology of the surface and the fracture cross-section of the specimens were observed by a field emission scanning electron microscope (FESEM: S-5000, Hitachi) with an energy dispersive X-ray analyzer after osmium evaporation. The UV–vis spectra of the specimens after anodization were measured by a spectrophotometer (U-3500, Hitachi).

### 3. Results and discussion

#### 3.1. Anodizing behavior

Fig. 2 shows the time variation in current density ( $i_a-t_a$ ) for the sputtered aluminum specimens anodized down to the ITO/glass substrate in various acid solutions. For all the specimens, the  $i_a-t_a$  curves exhibit a relatively stable region, corresponding to anodization of aluminum layer, and a large current fluctuation with gas evolution, corresponding to the electrolysis at the Al–ITO interface (see shadow areas). Accompanied by the characteristic current swings, the appearances of the specimens also change from opaque to transparent gradually, indicating the consumption of aluminum and the end of the anodization.

#### 3.2. Microstructures of anodic alumina films

Fig. 3 shows the FESEM images of the fracture sections for the specimens anodized down to the substrate obtained at the conditions in Fig. 2. Porous

alumina structures with straight and parallel channels perpendicular to the substrate are obtained for all the specimens. Particularly, the barrier layers of the anodic alumina films formed in the phosphoric acid solution

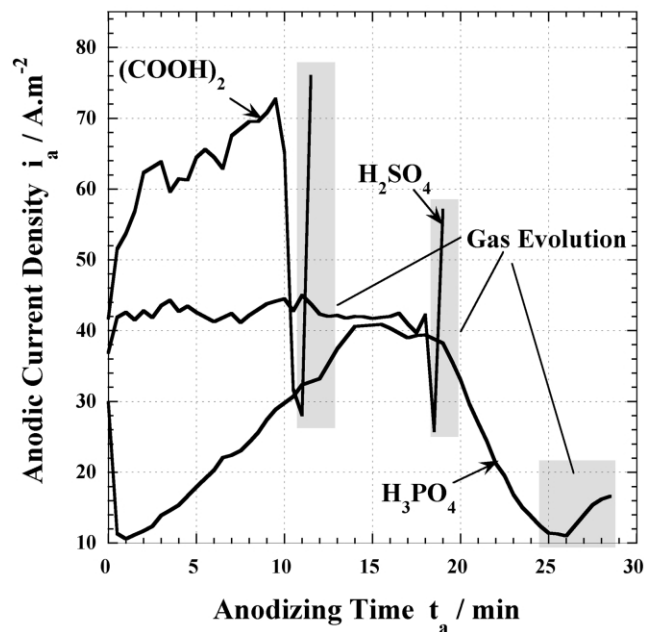


Fig. 2. Changes of current density ( $i_a$ ) with anodizing time ( $t_a$ ) for sputtered aluminum films anodized down to the ITO/glass substrate in solutions of 3% oxalic acid (40 V, 293 K), 10% sulfuric acid (15 V, 283 K), and 10% phosphoric acid (130 V, 280 K).

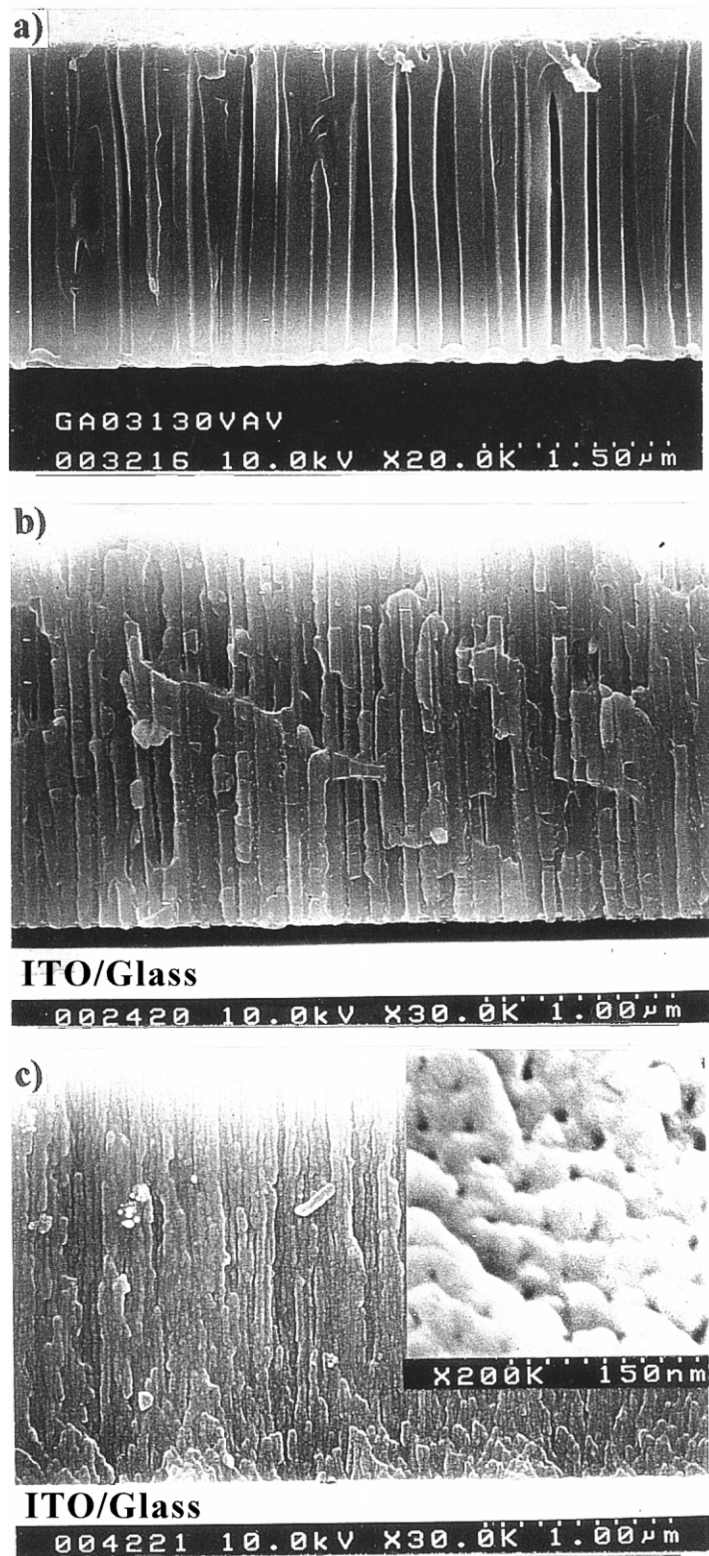


Fig. 3. FESEM images of vertical fracture sections of anodic alumina films formed in solutions of (a) phosphoric acid, (b) oxalic acid and (c) sulfuric acid. Insert in (c) is the transverse fracture section of the film. Anodizing conditions are the same as in Fig. 2.

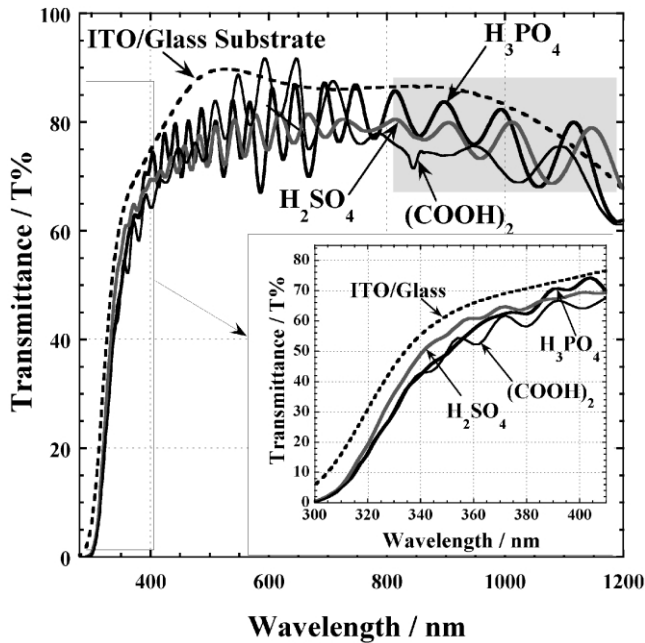


Fig. 4. UV-infrared transmittance spectra for the specimens anodized at different acid solutions. Anodizing conditions are the same as in Fig. 2.

(Fig. 3a) exhibit an arched shape with a thin thickness of  $1/4$ – $1/3$  of the pore walls, which may be caused by the local increases of temperature and/or acidity at the pore bases during anodization of the Al–ITO interface [6]. The average pore sizes and pore spacing of the anodic alumina films are approximately 150 and 350 nm, 30 and 100 nm, and 6 and 50 nm for phosphoric, oxalic and sulfuric acid solutions, respectively. Correspondingly, through appropriate chemical dissolutions, the pores can be widened to  $\sim \varnothing 200$ ,  $\sim \varnothing 50$  and  $\sim \varnothing 20$  nm, respectively.

### 3.3. Transparency of anodic alumina films

The transparency of materials is an important parameter for applications in photocatalysis and photocell systems. Fig. 4 shows the UV-infrared transmittance spectra for the specimens anodized in different solutions. The average transmittances of all the anodized specimens are close to that of the ITO/glass substrate (dot line), indicating that the alumina films are all transparent through UV–visible range, due to the consumption of aluminum by anodization. In visible light range, the interference patterns in the spectra are similar, irrespective of the pore size and the sort of the films; while in near infrared region (shadow area) and UV range (insert), the interference fluctuation in the spectra would infer some dependence upon the pore sizes and/or the sorts of alumina films.

### 3.4. Synthesis of titania nanostructures

In sol–gel process, the  $\text{TiO}_2$  is filled into the pores of the anodic alumina films driven by the capillary effect. Fig. 5 displays the fracture sections for the specimens after dip-coating in the  $\text{TiO}_2$  sol and heated at 673 K for 2 h. For the films formed in phosphoric acid solution (Fig. 5a), the  $\text{TiO}_2$  sol enters the nanopores along the walls of anodic alumina films and connects directly to the substrate. After being dried and heated, the  $\text{TiO}_2$  layer adheres to the pore walls because of its good affinity to the alumina film, thus forming a hollow  $\text{TiO}_2$ -coated nanostructure with a large surface area. For the oxalic-anodized alumina films (Fig. 5b), on the other hand, the resultant  $\text{TiO}_2$  is in the form of a solid structure with many voids inside and with poor adherence to the alumina wall (see arrows). As for the sulfuric-anodized film,  $\text{TiO}_2$  sol could not enter the pores of the films, probably because of the small pore

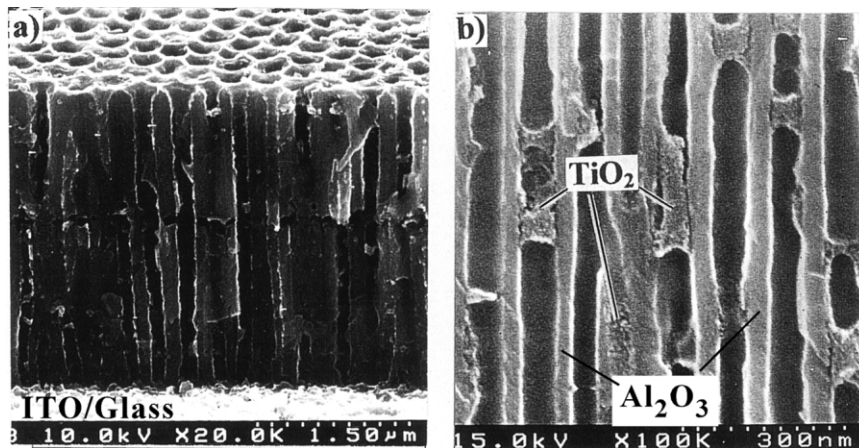


Fig. 5. FESEM images of fracture section for specimens dip-coated in a  $\text{TiO}_2$  sol and heated at 673 K for 2 h. Fabrication conditions: (a) 10%  $\text{H}_3\text{PO}_4$ , 150 V, 277 K,  $t_{p,w}=45$  min,  $t_{dip}=20$  min; (b) 3% oxalic acid, 40 V, 293 K;  $t_{p,w}=15$  min,  $t_{dip}=10$  min.

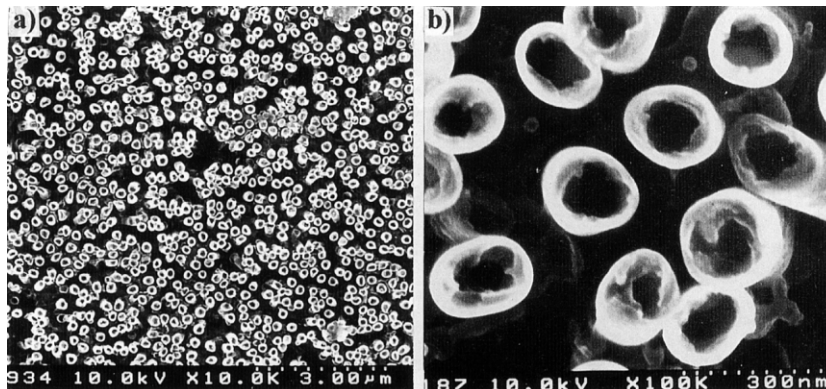


Fig. 6. Titania nanotubules array ( $\sim\varnothing 200\text{ nm}\times 40\text{ nm}\times 3\text{ }\mu\text{m}$ ) standing on an ITO/glass substrate (Anodization: 10%  $\text{H}_3\text{PO}_4$ , 150 V, 277 K; Pore-widening: 45 min).

size ( $\sim\varnothing 20\text{ nm}$ ) in the film and/or the viscosity and the surface tension of the  $\text{TiO}_2$  sol adopted.

Fig. 6 gives an example of  $\text{TiO}_2$  nanotubules array on the glass substrate. The  $\text{TiO}_2$  nanotubules,  $\sim\varnothing 200\text{ nm}$  for outer diameter,  $\sim\varnothing 40\text{ nm}$  thick and  $\sim 3\text{ }\mu\text{m}$  long, stand straight on the ITO/glass substrate with certain spaces among each other, thus giving a very large surface area that may be incomparable for conventional  $\text{TiO}_2$  layers. Moreover, according to XRD analysis and TEM observation (not shown), the  $\text{TiO}_2$  nanotubules are polycrystalline anatase and composed of 4–20 nm grains, which are known to be associated to the good photocatalytic performances.

#### 4. Conclusions

Various oxide nanostructures, highly porous alumina films ( $\varnothing 6\text{--}150\text{ nm}$ ) and  $\text{TiO}_2/\text{Al}_2\text{O}_3$  layers ( $\sim\varnothing 120\text{ nm}$ ), well-arranged  $\text{TiO}_2$  nanotubules arrays ( $\sim\varnothing 200\text{ nm}$ ), and  $\text{TiO}_2$  nanofibers ( $\sim\varnothing 50\text{ nm}$ ) on ITO/glass substrates were fabricated by combining techniques of

aluminum anodization and a sol–gel process. The resultant nanostructures, especially the porous  $\text{TiO}_2/\text{Al}_2\text{O}_3$  composite layers and  $\text{TiO}_2$  nanotubule arrays synthesized upon phosphoric-anodized films, possess large surface areas and are mechanically strong with good adherence to the substrate. Therefore, it is reasonable to consider the  $\text{TiO}_2$  nanostructures as a promising nanomaterial in the manufacture of practical devices for photocatalysis and photocells system, which are being explored.

#### References

- [1] C.R. Martin, *Science* 266 (1994) 1961.
- [2] B.B. Lakshmi, P.K. Dorhout, C.R. Martin, *Chem. Mater.* 9 (1997) 857.
- [3] R.C. Furneaux, W.R. Rigby, A.P. Davidson, *Nature* 337 (1989) 147.
- [4] H. Masuda, K. Fukuda, *Science* 268 (1995) 1466.
- [5] S.Z. Chu, K. Wada, S. Inoue, S. Todoroki, *Chem. Mater.* 14 (2002) 266.
- [6] S.Z. Chu, K. Wada, S. Inoue, S. Todoroki, *J. Electrochem. Soc.* 149 (7) (2002) B321.